3 Biotech (2021) 11:327
https://doi.org/10.1007/s13205-021-02865-x

ORIGINAL ARTICLE

Comparative transcriptome analysis of the hyperaccumulator plant *Phytolacca americana* in response to cadmium stress

Le Zhao[1,2] · Yun-Hao Zhu[1,2] · Min Wang[3] · Li-Gang Ma[1,2] · Yong-Guang Han[1] · Meng-Jia Zhang[1] · Xing-Can Li[1] · Wei-Sheng Feng[1,2] · Xiao-Ke Zheng[1,2]

Received: 28 March 2021 / Accepted: 31 May 2021 / Published online: 12 June 2021

Abstract

To study the molecular mechanism of the hyperaccumulator plant *Phytolacca americana* against cadmium (Cd) stress, the leaves of *P. americana* treated with 400 μM Cd for 0, 2, 12, and 24 h were harvested for comparative transcriptome analysis. In total, 110.07 Gb of clean data were obtained, and 63,957 unigenes were acquired after being assembled. Due to the lack of *P. americana* genome information, only 24,517 unigenes were annotated by public databases. After Cd treatment, 5054 differentially expressed genes (DEGs) were identified. KEGG pathway enrichment analysis of DEGs showed that genes involved in the flavonoid biosynthesis and antenna proteins of photosynthesis were significantly down-regulated, while genes related to the lignin biosynthesis pathway were remarkably up-regulated, indicating that *P. americana* could synthesize more lignin to cope with Cd stress. Moreover, genes related to heavy metal accumulation, sulfur metabolism and glutathione metabolism were also significantly up-regulated. The gene expression pattern of several key genes related to distinct metabolic pathways was verified by qRT-PCR. The results indicated that the immobilization of lignin in cell wall, chelation, vacuolar compartmentalization, as well as the increase of thiol compounds content may be the important mechanisms of Cd detoxification in hyperaccumulator plant *P. americana*.

Accession numbers: the raw data of *P. americana* transcriptome presented in this study are openly available in NCBI SRA database, under the BioProject of PRJNA649785.

Keywords *Phytolacca Americana* · Cadmium stress · Comparative transcriptome · Differentially expressed genes · Bioinformatics analysis

Abbreviations

Cd	Cadmium
4CL	4-Coumarate-CoA ligase
ANS	Anthocyanidin synthase
As	Arsenic
BP	Biological process
C4H	Trans-cinnamate 4-hydroxylase
CAD	Cinnamyl alcohol dehydrogenase
CC	Cellular component
CCM	Carbon dioxide concentration Mechanism
CCoAOMT	Caffeoyl-CoA O-methyltransferase
CDF	Cation diffusion facilitator
CHI	Chalcone isomerase
CHS	Chalcone synthase
COG	Clusters of orthologous groups
COMT	Caffeic acid 3-O-methyltransferase
Cr	Chromium
Cu	Copper
CYP75B1	Flavonoid 3-monooxygenase
Cys	Cysteine
DEG	Differentially expressed gene
DFR	Dihydroflavonol 4-reductase
EF	Enrichment factor
F3H	Flavanone 3-hydroxylase
F5H	Ferulate-5-hydroxylase
FC	Fold change

✉ Xiao-Ke Zheng
zhengxk.2006@163.com

[1] School of Pharmacy, Henan University of Chinese Medicine, No. 156 Jinshui East Road, Zhengzhou 450046, Henan, China

[2] Collaborative Innovation Center for Respiratory Disease Diagnosis and Treatment and Chinese Medicine Development of Henan Province, Zhengzhou 450046, China

[3] Beijing Key Laboratory of Plant Research and Development, College of Chemistry and Materials Engineering, Beijing Technology and Business University, Beijing 100048, China

FDR	False discovery rate
FLS	Flavonol synthase
FPKM	Fragments per kilobase of transcript per million mapped reads
GO	Gene ontology
GSH	Glutathione
GST	Glutathione S-transferase
HCT	Shikimate O-hydroxycinnamoyl transferase
Hcy	Homocysteine
Hg	Mercury
HMA3	Heavy metal ATPase 3
HMA5	Heavy metal ATPase 5
ICP-ES	Inductive coupled plasma emission spectrometry
JA	Jasmonic acid
KEGG	Kyoto encyclopedia of genes and genomes
KOG	EuKaryotic orthologous groups
LAR	Leucoanthocyanidin reductase
LHC	Light-harvesting complex
MAT	S-adenosylmethionine synthase
MEP	Ministry of environmental protection
Met	Methionine
MetE	Cobalamin-independent methionine synthase
MF	Molecular function
MLR	Ministry of land and resources
Mn	Manganese
MT	Metallothionein
MT3	Metallothionein-like protein type 3
MTP	Metal tolerance protein
NA	Nicotianamine
NAS	Nicotianamine synthase
Ni	Nickel
Nr	Non-redundant
NRAMP3	Natural resistance-associated macrophage protein 3
PA	Polyamine
PAL	Phenylalanine ammonia lyase
Pb	Lead
PC	Phytochelatin
PCS	Phytochelatin synthase
Pfam	Protein family
POX	Plant peroxidase
PRDX6	Peroxiredoxin 6
qRT-PCR	Quantitative real-time PCR
ROS	Reactive oxygen species
SAM	S-adenosylmethionine
SAT1	Serine acetyltransferase 1
SSH	Suppression subtractive hybridization
Zn	Zinc
ZNT1	Zn transporter 1
ZNT4	Zn transporter 4

Introduction

Cadmium (Cd), as a non-essential element in the biological development, does not have any biological functions and is highly toxic to most organisms. Due to human activities, such as the application of phosphate fertilizer, metallurgical industry, and production of nickel-Cd batteries, etc., it is estimated that approximately 30,000 tons of Cd are discharged into the atmosphere each year worldwide (Gallego et al. 2012; Luo et al. 2016). Cd is highly mobile, soluble, and easily accumulates in plant tissues which grow in Cd contaminated soil. Eventually, Cd can enter the human body through the food chain. Cd at a very low concentration can be carcinogenic and poses a serious threat to the health of the human body (Bertin and Averbeck 2006; Satarug et al. 2010).

In China, according to the "National Soil Pollution Survey Bulletin" jointly issued by the Ministry of Environmental Protection (MEP) and the Ministry of Land and Resources (MLR) in 2014, the Cd pollutant sites exceeded the standard rate at 7.0%, and ranked first among the 8 inorganic pollutants (Cd, mercury (Hg), arsenic (As), copper (Cu), lead (Pb), chromium (Cr), zinc (Zn), nickel (Ni)) (MEP and MLR 2014). Therefore, the problem of soil Cd pollution is increasing not only in China, but also in the world, and it has become an environmental issue that the public is deeply concerned about and urgently needs to solve. The physical, chemical, and biological remediation methods are the most common methods for Cd contaminated soil, but physical and chemical remediation methods require a lot of manpower and financial resources. Phytoremediation is therefore one of the most promising and cost-effective biological remediation methods for Cd contaminated soil, which mainly uses hyperaccumulator plants to transfer Cd from contaminated soil to the aerial parts of plants (Pilon-Smits 2005).

Hyperaccumulator plants are able to absorb large amounts of one or more heavy metals from the soil and transfer them to above-ground parts, such as leaves, without showing any symptoms of toxicity (Rascio and Navariizzo 2011). At present, more than 450 species of plants are identified to be heavy metal hyperaccumulators (Verbruggen et al. 2009), but only a few species are Cd hyperaccumulator plants, such as *Viola baoshanensis* (Wei et al. 2004), *Sedum plumbizincicola* (Jiang et al. 2010), *Thlaspi caerulescens*, *Arabidopsis halleri*, and *Sedum alfredii* (Krämer 2010). The slow growth rate and small biomass of these plants hinder the large-scale application of phytoremediation technology.

Phytolacca americana L. (also called pokeweed) belongs to the Phytolaccaceae family and is a perennial plant which often grows in heavy metal contaminated

mining areas (Liu et al. 2010). The previous reports showed that *P. americana* can accumulate a large amount of Cd and manganese (Mn) in its aerial parts. *P. americana* growing in heavy metal contaminated soils can accumulate up to 402 mg kg^{-1} of Cd and 13 900 mg kg^{-1} of Mn (Peng et al. 2008) in its leaves (Gao et al. 2013), which were significantly higher than the criterion of Cd and Mn hyperaccumulator plants (Cd > 100 mg kg^{-1}, Mn > 10,000 mg kg^{-1}) (Krämer 2010). In addition to the ability to accumulate large amounts of Cd, *P. americana* also has the advantage of rapid growth and large biomass. In the wild, the 1-year-old *P. americana* can grow up to 1–2 m. These significant advantages enable *P. americana* to be a promising and valuable plant species for both Cd phytoremediation and the study of molecular mechanisms in Cd hyperaccumulation.

Previous reports about the *P. americana* in response to Cd stress mainly focused on the physiological level (Gao et al. 2013; McBride and Zhou 2019), as well as subcellular distribution and chemical forms of Cd (Fu et al. 2011), while there are few reports on the molecular mechanism of *P. americana* in response to Cd stress. Zhao et al. (2011) reported the changes in leaf proteome of *P. americana* under Cd stress and found the significant changes that occurred in the proteins of both photosynthetic pathways and the sulfur and glutathione (GSH) related metabolic pathways. Zhao et al. (2019) used suppression subtractive hybridization (SSH) method to obtain 447 ESTs in *P. americana* after Cd treatment, and *PaGST*, *PaFe-SOD* as well as *PaMT* genes were expressed in yeast, which can improve the tolerance of yeast to Cd. Currently, there are few reports about large-scale sequencing of *P. americana* transcriptome. Neller et al. (2016) studied the transcriptome changes of *P. americana* leaves after jasmonic acid (JA) treatment and found that the differentially expressed genes (DEGs) were mainly stress-related genes and antiviral protein genes. Chen et al. (2017) conducted transcriptome analysis on Cd-treated *P. americana* (for 15 d) and control, obtained a total of 1,515 DEGs, and then analyzed the function of these DEGs.

In this study, we investigated the transcriptome changes of *P. americana* leaves at 0, 2, 12, 24 h after Cd treatment, and the results indicated that the significant changes took place in the expression of genes involved in sulfur and GSH metabolism, as well as heavy metal transporters. Meanwhile, after Cd treatment, the flavonoid biosynthesis was remarkably inhibited, whereas phenylpropanoid biosynthesis was significantly up-regulated through KEGG (Kyoto Encyclopedia of Genes and Genomes) pathway enrichment analysis, indicating that these metabolic pathways may be important for *P. americana* to cope with Cd stress.

Materials and methods

Plant material and Cd treatment

Seeds of *P. americana* were collected from Funiu Mountain National Nature Reserve in Henan province, China. The seeds were surface sterilized with sulfuric acid (98%) and ethanol (70%), each for 15 min, then placed on the 1/2 MS medium (Murashige and Skoog 1962). The seeds germinated and grew in a plant growth chamber with 16 h/23 ℃ light 8 h/20 ℃ dark for 21 d. After seeds germination, the seedlings were transplanted to a vessel containing 1/2 Hoagland solution (Hoagland and Arnon 1950) and grew for additional 21 days. The 1/2 Hoagland solution was changed every 2 days and, in each treatment, there were three independent biological replicates. The Cd treatments were 0, 100, 200, 400, 800 μM supplied with $CdCl_2$ in the 1/2 Hoagland solution. The leaves of *P. americana* were harvested at 0, 2, 12 and 24 h after Cd treatment, which were used for RNA extraction and further assay.

Cd, chlorophyll, and water content in *P. americana*

The leaves of *P. americana* were washed with distilled water, dried at 105 °C for 48 h, then dried at 65 °C to constant weight. The samples were ground into powder, then 50 mg powder was digested with 68% nitric acid at 60 °C for 48 h. The digested solution was diluted with ultrapure water (1:20), then the content of the Cd was determined by ICP-ES (Inductive Coupled Plasma Emission Spectrometry) (Thermo 6300, USA) (Gong et al. 2003). The chlorophyll content was measured using the Arnon method (Arnon 1949), and the water content was detected according to Jin's paper (Jin et al. 2017).

Determination of photosynthetic parameters

The true leaves at the base of *P. americana* were selected, and LI-6400 Portable Photosynthesis System (LI-COR, USA) was used to detect the changes of photosynthetic parameters from 0 to 72 h after 400 μM Cd treatment. Photosynthetic parameters such as photosynthetic rate, stomatal conductance, intercellular CO_2 concentration, and transpiration rate were measured.

RNA extraction, cDNA library construction and Illumina sequencing

Total RNA of different samples was extracted using TRIzol reagent (Invitrogen, USA) according to manufactory's instructions. The purity, concentration, and completeness

of RNA samples were detected by Nanodrop, Qubit 3.0, and Aglient 2100 respectively, to ensure that the RNA quality met the requirements of Illumina sequencing.

The cDNA library construction and RNA-seq were performed by the BioMarker Technologies Corporation (Beijing, China). The main process of cDNA library was as follows: (1) The mRNA was enriched with Oligo (dT) magnetic beads; (2) The mRNA was randomly broken into short fragments with fragmentation buffer; (3) The first cDNA strand was synthesized using random hexamers primer, and then the second cDNA strand was synthesized using DNA polymerase I, dNTPs and RNase H. The double-strand cDNA was purified with AMPure XP beads; (4) The purified double-strand cDNA was performed with end reparation, adding "A" tail and ligation to the sequencing adaptors, and then AMPure XP beads were used for fragment size selection; (5) The purified cDNA template was enriched with PCR amplification. Finally, the 12 cDNA libraries were constructed and sequenced using Illumina HiSeq 4000 platform. Each sample obtained no less than 7 Gb clean data from RNA-seq.

Assembly and functional annotation of RNA-seq data

To obtain high quality clean data, the sequencing primers, sequencing adaptors, repeat sequences, and low quality reads were removed from the raw data. The clean data were de novo assembled with Trinity software (Grabherr et al. 2011), and the contigs, transcripts and unigenes were obtained after assembling.

The all unigene sequences were aligned with NCBI nonredundant (Nr), Swiss-Prot, Gene Ontology (GO), Clusters of Orthologous Groups (COG), euKaryotic Orthologous Groups (KOG) and KEGG databases using BLAST program (E value $< 10^{-5}$). The KOBAS 2.0 software (Xie et al. 2011) was used to obtain unigene KEGG orthology results in KEGG pathway. The predicted amino acid sequences of unigenes were aligned with Protein family (Pfam) database using HMMER software (Eddy 1998) (E value $< 10^{-10}$) to acquire unigene annotation information.

Differential expression genes analysis

To analyze the DEGs, the Bowtie software (Langmead et al. 2009) was applied to align the reads of each sample with unigene library. According to the alignment results, the gene expression levels were normalized using FPKM (fragments per kilobase of transcript per million mapped reads) value (Trapnell et al. 2010). In statistical analysis, the Benjamini–Hochberg method was adopted and the corrected p value, i.e., false discovery rate (FDR), was used as the key factor for DEGs screening. The FDR < 0.01 and the fold change (FC) ≥ 2 were set as the threshold in the screening process. The volcano plot was a type of scatter plot, which combined the statistical significance (FDR) with the magnitude of change (FC). It can help to quickly identify those genes with large fold changes and statistical significance. The abscissa was represented by log2 (FC) and the ordinate was represented by − log10 (FDR). The genes in the upper left and upper right parts of the volcano plot were the most statistically significant DEGs with the largest fold changes. The BLAST2GO software was applied to analyze the functional GO enrichment of DEGs. Meanwhile, the KEGG pathway enrichment analysis of DEGs was carried out using KOBAS 2.0 software. The enrichment degree of the KEGG pathway was analyzed using the enrichment factor (EF), and the significance of enrichment was calculated by the Fisher's exact test.

Quantitative real-time PCR (qRT-PCR) verification

Several stress-related genes were selected to verify the expression levels of RNA-Seq by qRT-PCR. The total RNA was extracted from 100 mg sample using RNAprep Pure Plant Kit (Tiangen, Beijing) according to manufacturer's instructions. The first cDNA strand was synthesized from 200 ng total RNA using TransScript II Reverse Transcriptase (Transgene, Beijing). The cDNA diluted 10 times was used as the template of qRT-PCR and TUBLIN-α was used as reference gene (Zhao et al. 2019; Wang et al. 2012). The sequences of primers applied in qRT-PCR were listed in Suppl Table 1. Based on the manufacture's protocol, QuantiNova SYBR Green PCR kit (Qiagen, Germany) was adopted for qRT-PCR analysis and the qRT-PCR was run on Applied Biosystems QuantStudio 5 system (ABI, USA). Each sample had three independent biological replicates and the relative expression levels were calculated using $2^{-\Delta\Delta CT}$ method (Livak and Schmittgen 2001). The experimental data were analyzed with SPSS 16.0 software for one-way *ANOVA* test.

Statistical analysis

The experimental data were analyzed by Excel 2019 and SPSS 16.0 software, and the data were expressed as the mean ± standard deviation ($\bar{x} \pm s$). The data between the treatment group and the control group were compared by one-way *ANOVA* test, of which $p < 0.05$ showed a significant difference indicated by "*", and $p < 0.01$ represented an extremely significant difference indicated by "**".

Results

Effect of Cd on the growth of *P. americana*

When *P. americana* was treated with 100, 200, and 400 μM Cd for 24 h, there was no significant difference in leaf

morphology, chlorophyll content and water content between the treatment and the control (Fig. 1a, b, c). However, when *P. americana* was treated with 800 µM Cd for 24 h, the chlorophyll content of the leaves decreased from 1.75 mg g^{-1} FW to 1.54 mg g^{-1} FW ($p < 0.05$) compared to the control (Fig. 1b), the water content decreased from 93.7 to 92.6% ($p < 0.05$) (Fig. 1c), and the leaf margins began to show slight chlorosis under Cd stress (Fig. 1a), which indicated that 800 µM Cd severely repressed the growth of *P. americana*.

To confirm that *P. americana* was a hyperaccumulator plant of Cd, the Cd content in the leaves was determined under different Cd concentration treatment. The results indicated that the accumulation of Cd in leaves increased remarkably with the increase of Cd concentration (Fig. 1d). Under 400 µM Cd treatment, 200 mg kg^{-1} DW Cd ($p < 0.01$) can be accumulated in the leaves of *P. americana* (Fig. 1d), which was significantly higher than the standard of Cd hyperaccumulator plants (100 mg kg^{-1} DW) (Krämer 2010). Meanwhile, *P. americana* showed no symptoms of Cd toxicity, and had the advantages of rapid growth and large biomass, indicating that *P. americana* was a potential hyperaccumulator plant for the remediation of Cd contaminated soil (Liu et al. 2010; Zhao et al. 2019).

The photosynthesis of plants was inhibited under Cd stress. There was no significant difference in photosynthetic parameters between Cd treatment and control at 2 h after Cd treatment. However, from 2 to 48 h, the photosynthetic rate, stomatal conductance, and transpiration rate of the *P. americana* decreased rapidly, and the intercellular CO_2 concentration decreased slightly (Fig. 2). At 48 h, compared with the control, the Cd treatment group showed significant differences ($p < 0.05$ or $p < 0.01$). The photosynthetic rate, stomatal conductance, and transpiration rate of the Cd treatment group were 17.90, 9.55, and 12.28% of the control, respectively (Fig. 2), which indicated that the photosynthesis of *P. americana* was seriously inhibited under Cd stress. From 48 to 72 h, the inhibited photosynthesis began to recover. At 72 h, the photosynthetic rate, stomatal conductance, and transpiration rate of the Cd treatment group were restored to 29.13, 16.93, and 23.22% of the control, respectively (Fig. 2), showing that *P. americana* could change the metabolic state and resume photosynthesis to cope with Cd stress. After 72 h, the leaves of *P. americana*

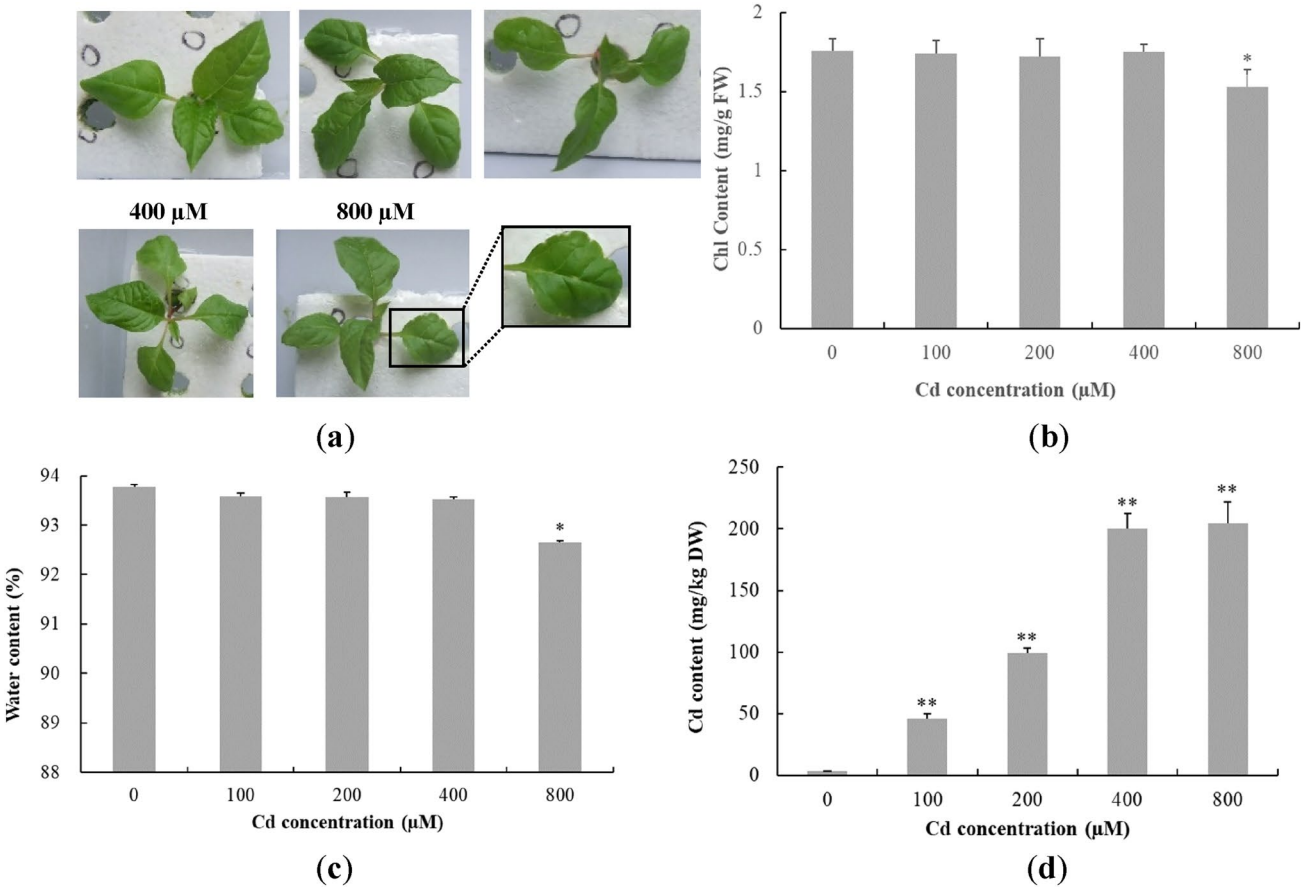

Fig. 1 The effect of Cd treatment with different concentrations for 24 h on the growth of *P. americana*. **a** leaf morphology, **b** leaf chlorophyll content, **c** leaf water content, **d** leaf Cd content. *$p < 0.05$, **$p < 0.01$, compared with controls

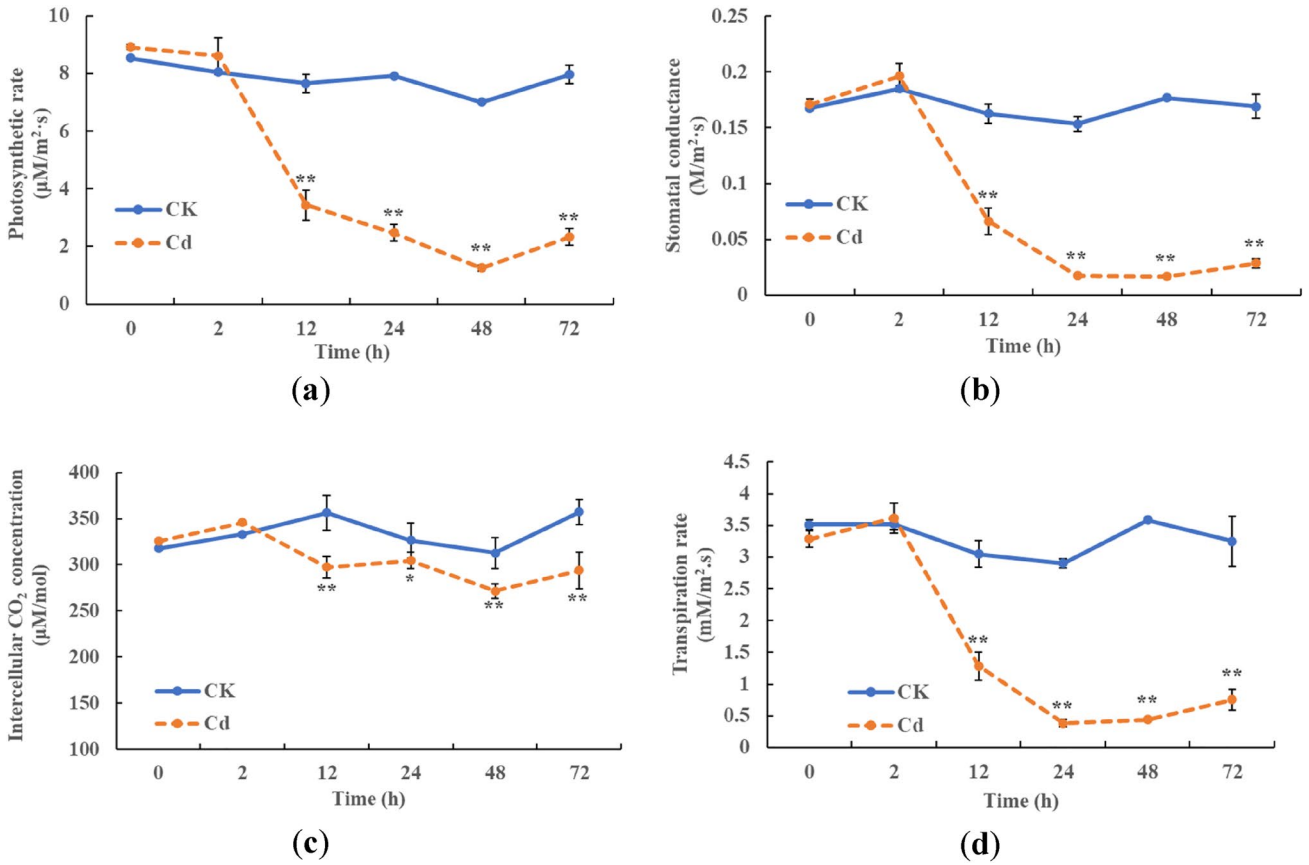

Fig. 2 Changes in photosynthesis parameters of *P. americana* under Cd treatment. **a** photosynthesis rate, **b** stomatal conductance, **c** intercellular CO_2 concentration, **d** transpiration rate. $*p<0.05$, $**p<0.01$, compared with controls

began to exhibit Cd toxic symptoms such as chlorosis, water loss, and wilting. To study the changes in gene expression of *P. americana* under Cd stress, the leaves of *P. americana* treated with 400 μM Cd for 0, 2, 12, and 24 h were harvested for further transcriptome analysis.

RNA-seq results and data assembly

After 400 μM Cd treatment, Illumina sequencing was performed on leaves of *P. americana* at 0, 2, 12, and 24 h, respectively, with 3 replicates of each sample. The transcriptomes of 12 samples were sequenced through Illumina Hiseq 4000 high throughput sequencing platform, and a total of 110.07 Gb of clean data were obtained. The clean data of each sample were at least 7.41 Gb, the average GC content was 46.36%, and the ratio of Q30 reached more than 89.02% (Table 1). After being assembled by Trinity software, 63,957 unigenes were obtained altogether, of which 19,321 unigenes were longer than 1 Kb. The average length of unigenes was 988.82 bp, and N50 of unigenes was 1541 bp (Suppl Fig. 1). Through alignment with NCBI Nr, Swiss-Prot, KEGG, COG, KOG, GO, and Pfam databases, a total of 24,517 unigenes with function annotation were acquired, accounting for 38.33% of all the unigenes. Because the genome of *P. americana* has not been sequenced, there was no genetic information of *P. americana* in the public database. Although 63,957 unigenes were obtained, only 38.33% of the unigenes were annotated. The raw data of *P. americana* transcriptome was uploaded to NCBI SRA database, under the BioProject of PRJNA649785.

Bioinformatics analysis of DEGs

The FPKM value represented the expression level of unigenes in each sample, and the screening threshold was set to FDR < 0.01 and FC ≥ 2. According to the FPKM value of unigenes in different samples, the DEGs were identified, and then GO, COG, KEGG classification as well as KEGG pathway enrichment analysis of DEGs were performed.

In total, 5054 DEGs were identified among the 63,957 unigenes. At 2 h of Cd treatment, there were 1548 DEGs, of which 648 were up-regulated and 900 were down-regulated; at 12 h, there were 3516 DEGs, with 1525 up-regulated and 1991 down-regulated; at 24 h, there were 2680 DEGs,

Table 1 Summary of *P. americana* transcriptome sequencing results

Samples [a]	Total base number	Clean read number	GC content	≥ Q30% [b]	Mapped reads[c]	Mapped ratio
0 h-1	9,602,387,872	32,470,764	46.28%	90.12%	24,454,062	75.31%
0 h-2	9,000,290,382	30,445,052	46.15%	89.40%	23,065,500	75.76%
0 h-3	8,278,461,514	28,043,518	46.74%	90.18%	21,250,086	75.78%
Cd 2 h-1	9,597,140,484	32,530,249	46.15%	90.84%	24,397,848	75.00%
Cd 2 h-2	9,621,209,170	32,611,497	46.33%	90.61%	24,437,563	74.94%
Cd 2 h-3	8,381,451,782	28,380,147	46.27%	90.62%	21,392,551	75.38%
Cd 12 h-1	8,355,412,196	28,316,278	46.23%	89.02%	21,085,478	74.46%
Cd 12 h-2	9,746,505,190	33,197,254	45.92%	91.05%	24,534,469	73.91%
Cd 12 h-3	7,409,513,910	25,078,145	47.03%	90.52%	18,832,626	75.10%
Cd 24 h-1	8,868,083,580	30,032,640	46.51%	90.69%	22,606,770	75.27%
Cd 24 h-2	9,827,102,390	33,334,868	46.36%	91.11%	24,960,853	74.88%
Cd 24 h-3	11,386,412,014	38,492,796	46.37%	90.93%	29,117,131	75.64%

[a]The control (0 h) and the 400 µM Cd treatment at 2 h (Cd 2 h), 12 h (Cd 12 h) and 24 h (Cd 24 h). Each sample had three replicates

[b]The percentage of bases with a clean data is equal to or greater than 30

[c]Mapped reads were the reads of clean data that can be aligned to the assembled transcriptome library

with 1141 up-regulated and 1539 down-regulated (Table 2, Fig. 3). As shown in Table 2, the identified DEGs were functionally annotated by different public databases. In the DEG sets between 0 h vs Cd 2 h, 0 h vs Cd 12 h, and 0 h vs Cd 24 h, 1213 (78.36%), 2632 (74.86%), and 2084 (77.76%) unigenes were annotated by the Nr database, respectively.

GO functional enrichment of DEGs

The GO database is a structural standard biological annotation system that establishes a standard vocabulary system to describe the functions of genes and their products, and the GO database can be applied to annotate gene functions of various species (Consortium 2004). The annotation results of DEGs between different samples and all unigenes in GO secondary function nodes were shown in Fig. 4. In total, 1492 DEGs with at least one annotation were obtained at 12 h after Cd treatment. These DEGs were classified into 3 categories, including biological process (BP), cellular component (CC), molecular function (MF), and 51 subcategories (Fig. 4), in which 4297 DGEs were annotated as BP, 2673 DEGs as CC, and 1790 DEGs as MF, respectively. As can be seen from Fig. 4, DEGs and all unigenes were annotated in the GO secondary function nodes. The GO classification of DEGs at 2 and 24 h after Cd treatment was shown in Suppl Fig. 2.

At 12 h after Cd treatment, the oxidation–reduction process (GO:0055114), photosynthesis—light harvesting (GO:0009765), phenylpropanoid metabolic process (GO:0009698) and lignin metabolic process (GO:0009808) showed significant enrichment in biological process; the apoplast (GO:0048046), plant-type cell wall (GO:0009505) and chloroplast part (GO:0044434) indicated significant enrichment in cellular component. These results indicated that these biological processes and cellular components of *P. americana* had undergone remarkable changes in response to Cd stress.

KEGG classification of DEGs

In organisms, different gene products coordinate with each other to perform biological functions. The KEGG database

Table 2 Number of DEGs with functional annotation in *P. americana*

DEG sets	All DEGs	Up-regulated DEGs[a]	Down-regulated DEGs[a]	Unchanged unigenes[a]	COG	GO	KEGG	KOG	Pfam	Swiss-Prot	Nr[b]
0 h vs Cd 2 h	1548	648	900	18,715	325	449	625	572	911	1200	1213
0 h vs Cd 12 h	3516	1525	1991	17,051	632	866	1329	1188	1882	2609	2632
0 h vs Cd 24 h	2680	1141	1539	17,667	531	755	1084	961	1543	2060	2084

[a]The number of DEGs identified by volcano plots from different DEG sets (Fig. 3)

[b]The number of DEGs annotated by different database

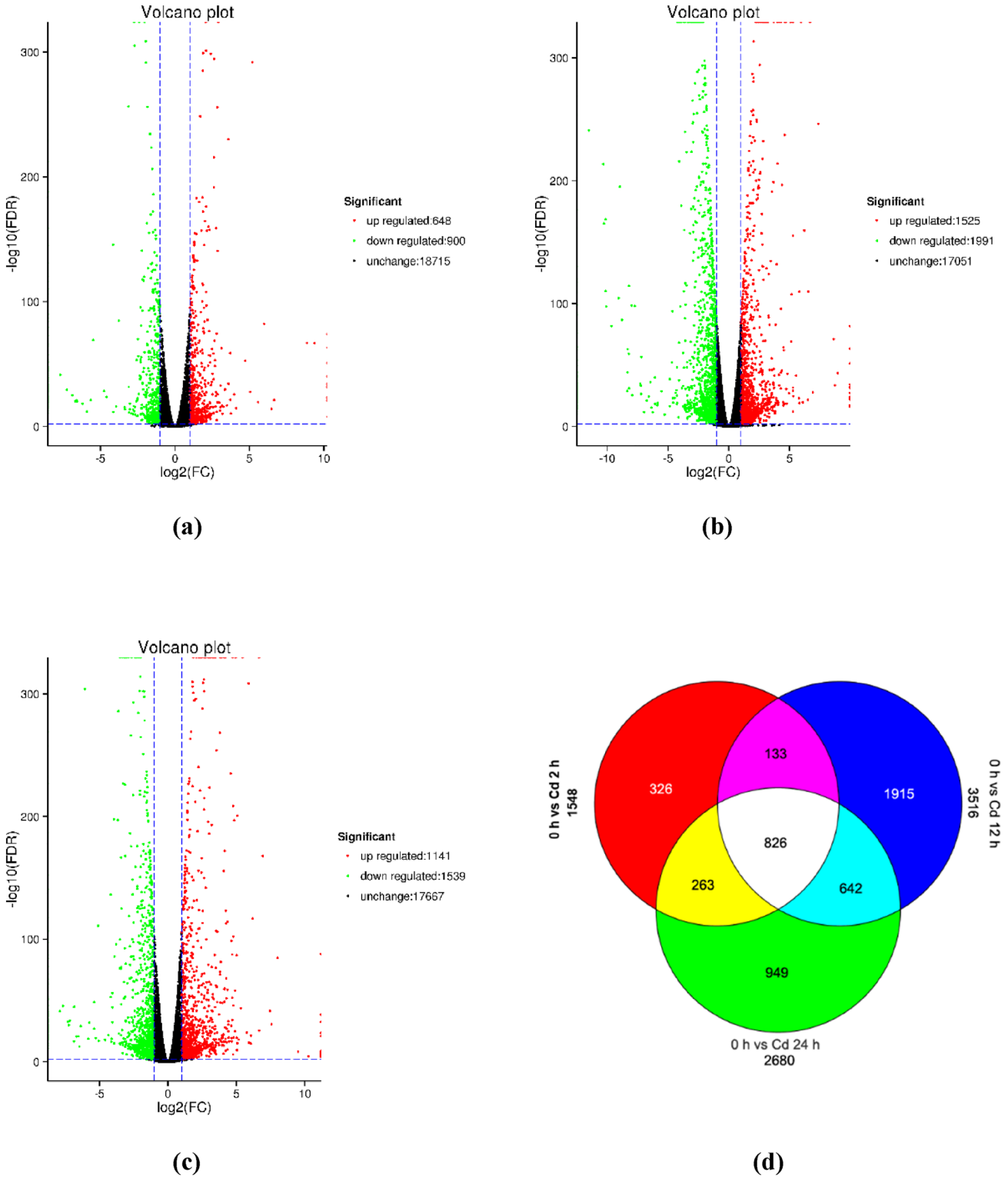

Fig. 3 Analysis of DEGs among 3 DEGs sets under Cd stress conditions. The volcano plots were constructed from 3 comparison groups, **a** 0 h vs Cd 2 h, **b** 0 h vs Cd 12 h, **c** 0 h vs Cd 24 h. Abscissa, log2(FC); ordinate, − log10 (FDR). Each point of volcano plots represents a gene, and the abscissa represents the differential expression level (FC) of a gene. The ordinate represents the significance of the DEGs. Green, down-regulated genes; red, up-regulated genes; black, genes with no significant differences. **d** venn diagram of DEGs in 3 comparison groups

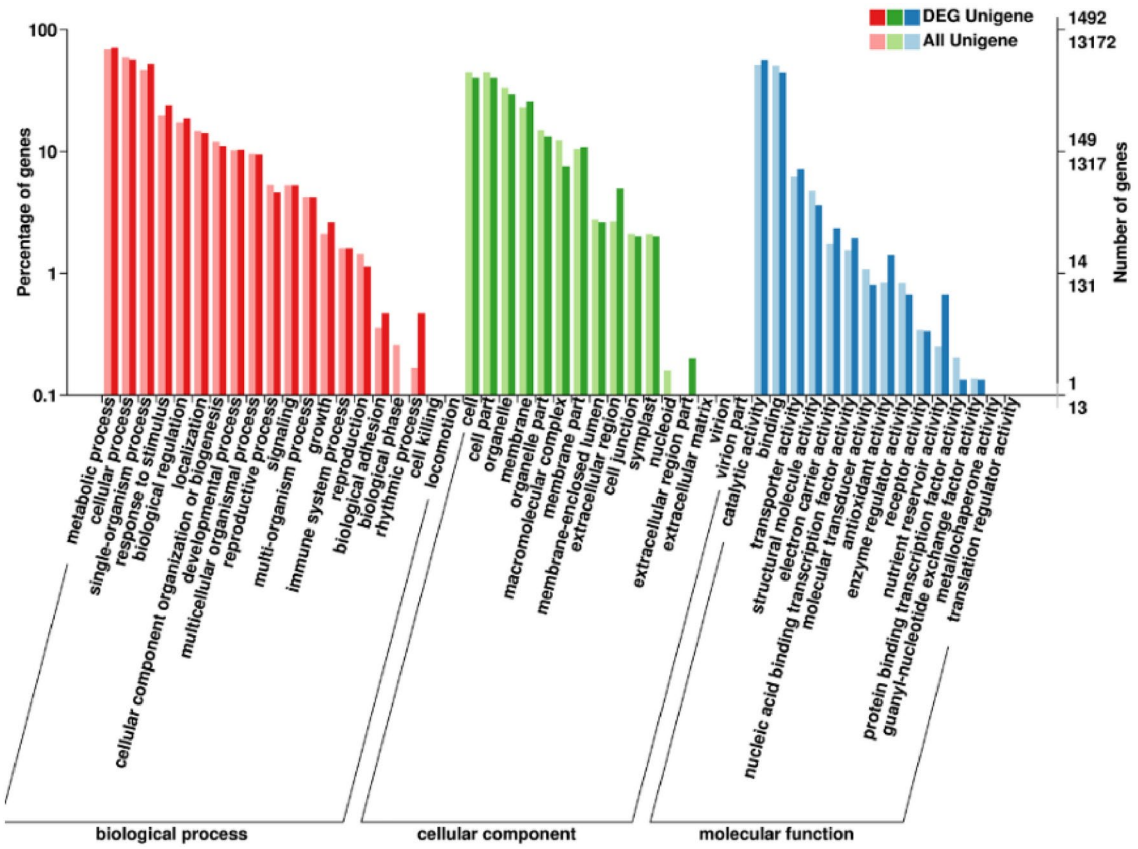

Fig. 4 GO enrichment analysis of DEGs for 0 h vs Cd 12 h. Abscissa, GO categories; ordinate (left), percentage of the number of genes; ordinate (right), the number of genes. The GO categories include biological processes, cellular components, molecular functions, and 51 subcategories

is the main public database on the pathway, and the annotation as well as analysis of DEGs' pathway contribute to further acquisition of gene functions (Kanehisa and Goto 2000). The annotation results of DEGs were classified according to the type of pathway in KEGG. Figure 5 showed the KEGG classification of DEGs at 12 h after Cd treatment, in which the metabolic pathways had the highest proportion (such as carbon metabolism, biosynthesis of amino acids, phenylpropanoid biosynthesis, and so on), followed by genetic information processing pathways (including ribosome, DNA replication, and RNA transport, etc.). The KEGG classification of DEGs at 2 h and 24 h after Cd treatment was shown in Suppl Fig. 3.

KEGG pathway enrichment analysis of DEGs

The KEGG pathway enrichment analysis of DEGs is to analyze whether DEG has over-presentation on a certain pathway. The enrichment factor (EF) was used to analyze the enrichment degree of metabolic pathways, and the Fisher's exact test (*P* value) was used to calculate the significance of enrichment. To detect the most significant KEGG pathway, the scatter plot of KEGG enrichment analysis of DEGs was constructed (Suppl Fig. 4). The EF was used as abscissa, and − log10 (*Q* value) was used as ordinate. EF is the ratio of numbers of DEGs annotated in this pathway to the numbers of all genes annotated in this pathway. The larger the EF, the higher degree of the enrichment. *Q* value, ranging from 0–1, is the corrected *P* value after multiple hypothesis test. The lower the *Q* value, the more significant of the enrichment. After Cd treatment, at different time point, the 5 most significant KEGG pathways of DEGs were shown in Table 3. Among them, flavonoid biosynthesis, phenylpropanoid biosynthesis and phenylalanine metabolism were the 3 most significant KEGG pathways, while photosynthesis—antenna proteins was detected at 12 h after Cd treatment (Table 3). Furthermore, the top 20 KEGG pathways with the most significant enrichment at different time point were displayed in Suppl Fig. 4.

Among them, genes involved in the flavonoid biosynthesis pathway were down-regulated (Table 4, Fig. 6a), including leucoanthocyanidin reductase (LAR), chalcone isomerase (CHI), flavonol synthase (FLS), and chalcone synthase (CHS). Other genes, such as flavanone-3-hydroxylase (F3H),

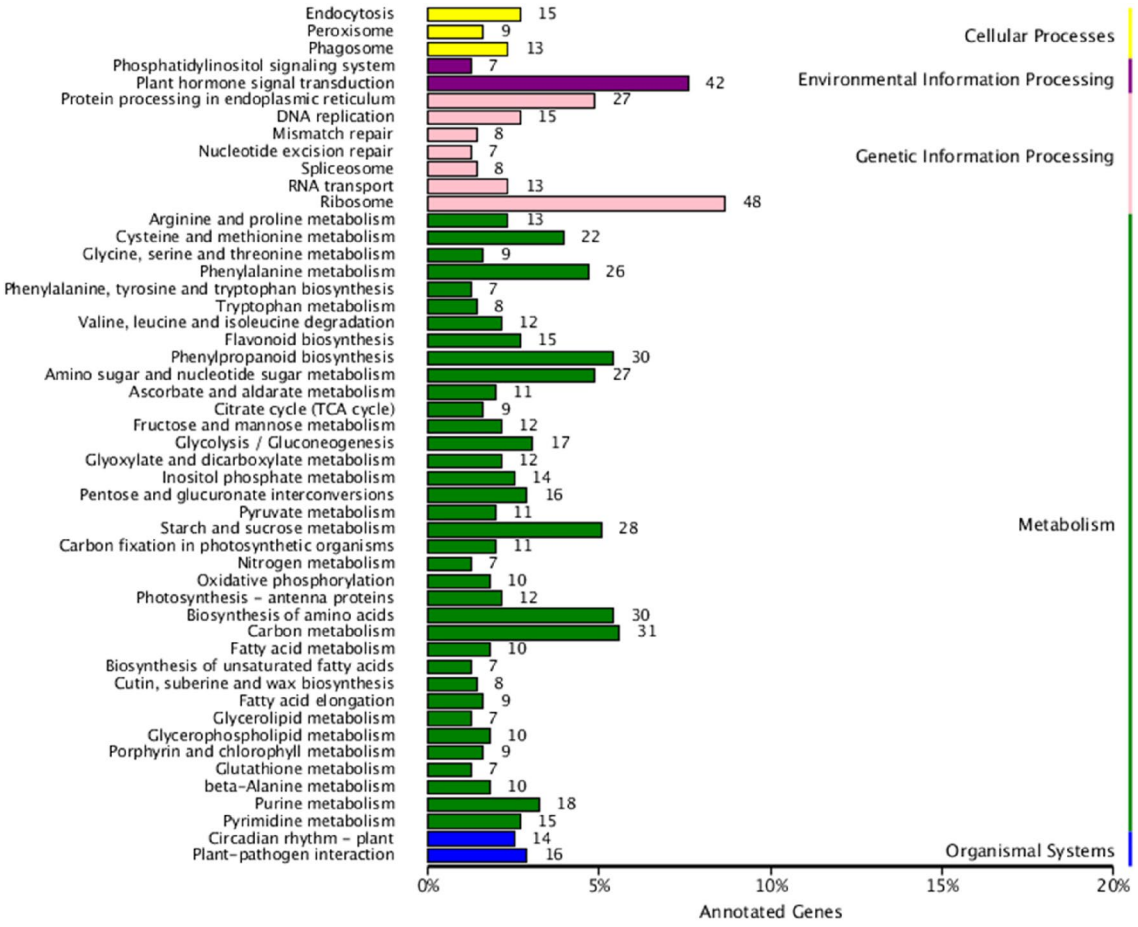

Fig. 5 KEGG classification of DEGs for 0 h vs Cd 12 h. Ordinate, the name of the KEGG pathway; abscissa, the number of genes annotated to the pathway and its proportion to the total number of genes annotated

Table 3 KEGG pathway enrichment analysis of DEGs

DEG sets	Pathway[a]	Ko ID[b]	Unigene number	*P* value[c]
0 h vs Cd 2 h	Flavonoid biosynthesis	Ko00941	16	3.79E–09
	Phenylpropanoid biosynthesis	Ko00940	23	9.74E–06
	Phenylalanine metabolism	Ko00360	17	1.46E–04
	Circadian rhythm—plant	Ko04712	10	5.38E–04
	Stilbenoid, diarylheptanoid and gingerol biosynthesis	Ko00945	6	1.13E–03
0 h vs Cd 12 h	Photosynthesis—antenna proteins	Ko00196	12	4.60E–07
	Phenylalanine metabolism	Ko00360	26	7.74E–05
	Flavonoid biosynthesis	Ko00941	15	9.91E–05
	Phenylpropanoid biosynthesis	Ko00940	30	4.78E–04
	Plant hormone signal transduction	Ko04075	42	5.89E–04
0 h vs Cd 24 h	Phenylpropanoid biosynthesis	Ko00940	38	3.17E–10
	Flavonoid biosynthesis	Ko00941	16	1.14E–06
	Phenylalanine metabolism	Ko00360	26	1.16E–06
	Stilbenoid, diarylheptanoid and gingerol biosynthesis	Ko00945	8	2.91E–04
	Cutin, suberine and wax biosynthesis	Ko00073	9	3.89E–04

[a]The 5 most significant KEGG pathways of DEGs (Suppl Fig. 4)

[b]KEGG pathways entry

[c]*P* value was obtained using clusterProfiler (R package) and the statistical method was Fisher's exact test

Table 4 DEGs involved in flavonoid biosynthesis and phenylpropanoid biosynthesis pathway

Gene name	Specific function	KO no. [a]	DEG unigene	Fold change[b]				Regulation
				0 h	2 h	12 h	24 h	
Flavonoid biosynthesis pathway								
Leucoanthocyanidin reductase (LAR)	LAR catalyzes the synthesis of catechin, which is an initiating monomer of condensed tannin or proanthocyanidin synthesis	K13081	c23232	1	0.48	0.20	0.30	Down
Chalcone isomerase (CHI)	CHI catalyzes the conversion of chalcone to flavanone, which is the second key enzyme in the biosynthesis of flavonoids	K01859	c57238	1	0.38	0.21	0.44	Down
			c63363	1	n.d.[c]	n.d	n.d	Diminished
Flavonol synthase (FLS)	FLS catalyzes the desaturation of dihydroflavonols to flavonols	K05278	c66981	1	0.39	0.48	0.55	Down
Chalcone synthase (CHS)	CHS is the first key enzyme in the biosynthesis of flavonoids	K00660	c58515	1	n.d	n.d	n.d	Diminished
			c64340	1	n.d	n.d	n.d	Diminished
			c74759	1	0.14	0.50	0.55	Down
Flavanone 3-hydroxylase (F3H)	F3H catalyzes an early step in the flavonoid biosynthesis pathway to produce flavanols and anthocyanins	K00475	c64120	1	n.d	n.d	n.d	Diminished

Table 4 (continued)

Gene name	Specific function	KO no. [a]	DEG unigene	Fold change[b]				Regulation
				0 h	2 h	12 h	24 h	
Flavonoid 3-monooxygenase (CYP75B1)	CYP75B1 is a plant cytochrome P450 protein that acts on many flavonoids, such as the flavanone naringenin and the flavone apigenin	K05280	c62847	1	n.d	n.d	n.d	Diminished
Anthocyanidin synthase (ANS)	ANS is involved in the formation of the anthocyanidins from leucoanthocyanidins	K05277	c59094	1	n.d	n.d	n.d	Diminished
Dihydroflavonol 4-reductase (DFR)	DFR is a key enzyme in the biosynthesis of anthocyanidins, which catalyzes the reduction of dihydroflavonols to produce leucoanthocyanidins	K13082	c75687	1	n.d	n.d	n.d	Diminished
Phenylpropanoid biosynthesis pathway								
Trans-cinnamate 4-hydroxylase (C4H)	C4H is a plant cytochrome P450 protein found in plants, which participates in phenylpropanoid biosynthesis	K00487	c28292	1	4.16	1.32	4.55	Up

Table 4 (continued)

Gene name	Specific function	KO no. [a]	DEG unigene	Fold change[b]				Regulation
				0 h	2 h	12 h	24 h	
Shikimate O-hydroxycinnamoyl transferase (HCT)	HCT catalyzes acyl group transfer, which is a central enzyme in the biosynthesis of monolignols	K13065	c43288	1	2.12	2.90	1.75	Up
Caffeic acid 3-O-methyltransferase (COMT)	COMT catalyzes the multi-step methylation reaction in lignin biosynthesis	K13066	c29912	1	4.75	6.74	14.94	Up
			c58030	1	2.40	1.37	1.63	Up
			c67663	1	4.57	6.72	14.55	Up
Ferulate-5-hydroxylase (F5H)	F5H is a key enzyme participated in the biosynthesis of sinapyl (S) monolignols	K09755	c58606	1	2.80	1.80	1.41	Up
Plant peroxidase (POX)	POX, a plant specific oxidoreductase, belongs to class III peroxidase, and catalyzes oxidoreduction reaction between H_2O_2 and reductants. POX is involved in response to oxidative stress	K00430	c55840	1	4.23	2.43	2.32	Up
			c58668	1	2.15	1.79	2.08	Up
			c66179	1	6.43	2.08	6.73	Up
			c68488	1	2.17	2.39	1.64	Up
			c70791	1	2.48	1.29	1.86	Up

Table 4 (continued)

Gene name	Specific function	KO no. [a]	DEG unigene	Fold change[b]				Regulation
				0 h	2 h	12 h	24 h	
Cinnamyl alcohol dehydrogenase (CAD)	CAD catalyzes the reduction of cinnamaldehyde to cinnamyl alcohol, the final step of monolignol biosynthesis	K00083	c59540	1	2.38	2.77	17.97	Up
4-coumarate-CoA ligase (4CL)	4CL takes part in the biosynthesis of monolignol by catalyzing the formation of *p*-coumaroyl-CoA	K01904	c62437	1	1.19	1.39	2.62	Up
			c60024	1	1.30	1.04	2.68	Up
Caffeoyl-CoA O-methyltransferase (CCoAOMT)	CCoAOMT is a key enzyme in the biosynthesis of lignin, which catalyzes the methylation of 3-hydroxyl group of caffeoyl-CoA to produce feruloyl-CoA	K00588	c67535	1	1.90	2.18	2.13	Up
Peroxiredoxin 6 (PRDX6)	PRDX6 catalyzes H_2O_2 detoxification through the Cys[d] residues	K11188	c47660	1	n.d	n.d	n.d	Diminished

[a]KEGG Orthology (KO) entry

[b]Fold change in comparison with FPKM value at 0 h

[c]Not detected (n.d.) after 400 µM Cd treatment

[d]*Cys* cysteine

flavonoid-3-monooxygenase (CYP75B1), anthocyanidin synthase (ANS), and dihydroflavonol 4-reductase (DFR), were not detected after Cd treatment. The results indicated that the biosynthesis of flavonoids was inhibited under Cd stress.

However, the genes involved in the phenylpropanoid biosynthesis pathway, especially those in lignin biosynthesis, were up-regulated under Cd treatment (Table 4, Fig. 6b), such as trans-cinnamic 4-hydroxylase (C4H), shikimate O-hydroxycinnamoyl transferase (HCT), caffeic acid 3-O-methyltransferase (COMT), ferulate-5-hydroxylase (F5H), plant peroxidase (POX), cinnamyl alcohol dehydrogenase (CAD), 4-coumarate-CoA ligase (4CL), and caffeoyl-CoA O-methyltransferase (CCoAOMT). These key enzyme genes involved in the lignin biosynthesis pathway were significantly up-regulated, indicating that *P. americana* could promote lignin biosynthesis to cope with Cd stress.

At 12 h after Cd treatment, however, the most significant KEGG pathway was photosynthesis-antenna proteins, followed by the phenylalanine metabolism, flavonoid biosynthesis, and phenylpropanoid biosynthesis (Table 3, Suppl Fig. 4b). Antenna proteins of photosynthesis, especially the light-harvesting complex (LHC) of photosystem I and photosystem II, 11 DEGs were significantly down-regulated at 12 h after Cd treatment (Fig. 6c, Suppl Fig. 5). Although the expression levels of *LHC* genes increased at 24 h, they were still lower than the control (Fig. 6c). The results indicated that the photosynthesis of *P. americana* was remarkably inhibited by Cd treatment. This inhibition may result from the suppression of *LHC* genes expression, which was also consistent with the previous detection of Cd treatment inhibiting the photosynthesis of *P. americana* (Fig. 2).

In response to Cd stress, the genes related to heavy metal accumulation and tolerance were significantly up-regulated (Table 5, Fig. 6d), such as Heavy metal ATPase 3 (HMA3), Heavy metal ATPase 5 (HMA5), metallothionein-like protein type 3 (MT3), natural resistance-associated macrophage protein 3 (NRAMP3), metal tolerance protein (MTP), phytochelatin synthase (PCS), and nicotianamine synthase (NAS), while Zn transporter 1 (ZNT1) and Zn transporter 4 (ZNT4) were down-regulated. Moreover, the genes involved in sulfur and glutathione metabolism were up-regulated (Table 5), including serine acetyltransferase 1 (SAT1), S-adenosylmethionine synthase (MAT), cobalamin-independent methionine synthase (MetE), and glutathione S-transferase (GST), and these genes were also important to cope with Cd stress in the *P. americana*.

qRT-PCR verification

To further verify the reliability of gene changes in comparative transcriptome analysis, several key genes related to distinct metabolic pathways were analyzed by qRT-PCR. As shown in Fig. 7, the alteration pattern of these genes was consistent with that of transcriptome analysis, indicating that the DEGs identified by comparative transcriptome analysis were reliable. The genes related to flavonoid biosynthesis and photosynthesis-antenna proteins, such as *FLS*, *LHCB1* and *LHCB5* were significantly down-regulated, whereas some genes involved in phenylpropanoid biosynthesis and heavy metal accumulation and tolerance, such as *POX*, *CAD*, *GST*, *MT3*, *HMA3*, *HMA5* and *NRAMP3* were remarkably up-regulated in *P. americana* after Cd treatment (Fig. 7).

Discussion

Effect of Cd on the growth of *P. americana*

Cd, as a non-essential element, does not have any biological function in plant growth and development. So far, only Cd-specific carbonic anhydrase has been found in the marine diatom (*Thalassiosira Weisslogii*), which can replace Zn carbonic anhydrase under Zn-limited condition and plays a role in the carbon dioxide concentration mechanism (CCM) (Lane and Morel 2000). The growth and metabolism of plants can be inhibited by Cd at very low concentration (0.1–1 μM). The toxicity of Cd to plants is manifested in several aspects: in terms of morphology, Cd suppresses plant growth causing the leaves show chlorosis, curling, and other Cd toxic symptoms; in physiological aspect, photosynthesis and transpiration are inhibited by Cd, which also interferes with plant nutrition metabolism and causes oxidative stress (Qadir et al. 2014).

In this study, when treated with Cd at a concentration of ≤ 400 μM for 24 h, there was no significant difference in the growth of the above-ground part of *P. americana* compared with the control (Fig. 1a, b, c). The results showed that Cd at a concentration of 0 to 400 μM had no significant inhibition on the growth of *P. americana*. However, when the Cd concentration reached 800 μM, the leaf margins began to show Cd toxic symptoms-chlorosis (Fig. 1a), and the water content and chlorophyll content of leaves decreased compared with the control and 400 μM samples ($p < 0.05$) (Fig. 1b, c), This was consistent with our previous reports (Zhao et al. 2011), and similar symptoms of Cd toxicity were also observed in *Spinacia oleracea*, *Brassica napus* and *Thlaspi caerulescens* (Baryla et al. 2001; Fagioni and Zolla 2009). X-ray microscopic analysis showed that the expanded cells of leaf margins are more sensitive to Cd than the rest parts of the leaf. This may explain why chlorosis was initially observed at the leaf margins (Cosio et al. 2005).

Theoretically, as the concentration of Cd treatment increased, the Cd content in the leaves of *P. americana* also increased significantly. However, there is an absorption limit even for hyperaccumulator plant. The Cd content

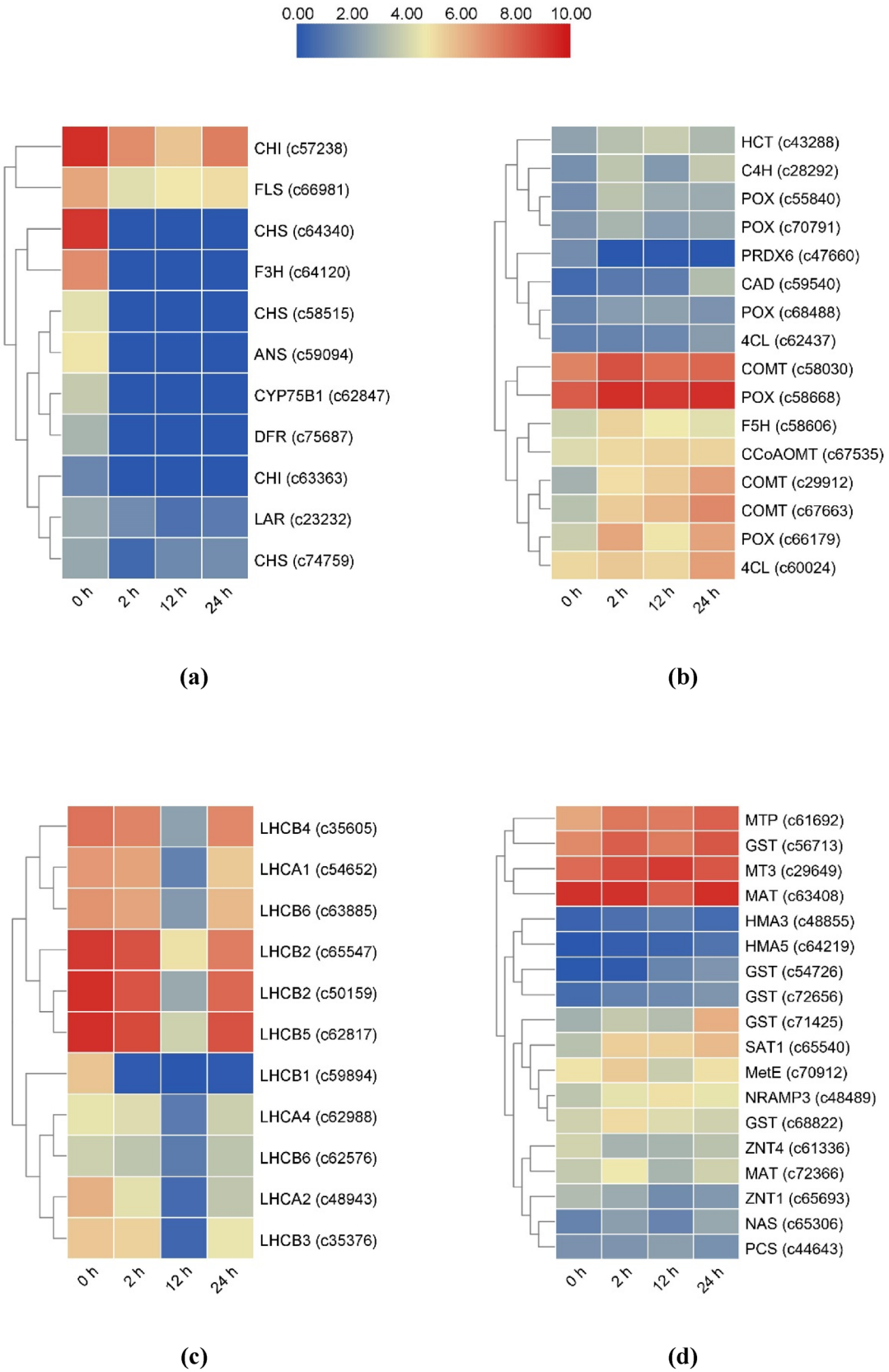
0.00 2.00 4.00 6.00 8.00 10.00
CHI (c57238)
FLS (c66981)
CHS (c64340)
F3H (c64120)
CHS (c58515)
ANS (c59094)
CYP75B1 (c62847)
DFR (c75687)
CHI (c63363)
LAR (c23232)
CHS (c74759)
0 h 2 h 12 h 24 h
(a)
HCT (c43288)
C4H (c28292)
POX (c55840)
POX (c70791)
PRDX6 (c47660)
CAD (c59540)
POX (c68488)
4CL (c62437)
COMT (c58030)
POX (c58668)
F5H (c58606)
CCoAOMT (c67535)
COMT (c29912)
COMT (c67663)
POX (c66179)
4CL (c60024)
0 h 2 h 12 h 24 h
(b)
LHCB4 (c35605)
LHCA1 (c54652)
LHCB6 (c63885)
LHCB2 (c65547)
LHCB2 (c50159)
LHCB5 (c62817)
LHCB1 (c59894)
LHCA4 (c62988)
LHCB6 (c62576)
LHCA2 (c48943)
LHCB3 (c35376)
0 h 2 h 12 h 24 h
(c)
MTP (c61692)
GST (c56713)
MT3 (c29649)
MAT (c63408)
HMA3 (c48855)
HMA5 (c64219)
GST (c54726)
GST (c72656)
GST (c71425)
SAT1 (c65540)
MetE (c70912)
NRAMP3 (c48489)
GST (c68822)
ZNT4 (c61336)
MAT (c72366)
ZNT1 (c65693)
NAS (c65306)
PCS (c44643)
0 h 2 h 12 h 24 h
(d)

◂**Fig. 6** Expression profiles clustering of DEGs related to different metabolic pathways. **a** flavonoid biosynthesis pathway, **b** phenylpropanoid biosynthesis pathway, **c** light-harvesting complex (LHC), **d** heavy metal accumulation and tolerance. Different columns represent different time points, and different rows represent different genes. The color represents the score value after FPKM normalization of the gene expression

in the leaves will not increase with the increase of the Cd concentration in the solution. We investigated the Cd content in *P. americana* leaves under 0, 100, 200, 400, 800, and 1000 μM Cd treatments at 24 and 48 h. (Suppl Fig. 6). The results showed that when the Cd concentration was 400, 800, 1000 μM, the Cd content in the leaves did not increase significantly, indicating that when the Cd concentration was higher than 400 μM, no more Cd would accumulate in *P. americana* leaves. Therefore, the 400 μM Cd concentration was chosen to treat *P. americana*, which was also the maximum Cd concentration that *P. americana* can tolerate.

The photosynthesis parameters of *P. americana* decreased rapidly after 2 h of Cd treatment and reached the lowest point at 48 h (Fig. 2). This was mainly due to the inhibition of photochemical activity and the decrease of chlorophyll content in chloroplasts (Šimonová et al. 2007; Yan et al. 2016). After 48 h, the photosynthesis of *P. americana* began to restore, but the degree of restoration was smaller. Although the stomatal conductance and transpiration rate were not much different between 24 and 48 h, these changes of photosynthetic parameters were related to physiological level. Gene transcription was a rapid response process, and its initiation should occur before the phenotype, so the changes of gene transcription level must be earlier than 48 h. These results indicated that the defense mechanism of *P. americana* against Cd stress was activated within the first 24 h. Therefore, we harvested leaves at 0, 2, 12, and 24 h after Cd treatment for comparative transcriptome analysis to study the molecular mechanism of *P. americana* against Cd stress.

By analyzing the transcriptome data, it was found that the expression levels of LHCA1, LHCA2, LHCA4 and LHCB1, LHCB2, LHCB3, LHCB4, LHCB5, LHCB6 corresponding to 11 DEGs were significantly down-regulated at 12 h after Cd treatment (Fig. 6). In addition, Cd can not only inhibit the expression of *LHC* gene, but also replaced Mg^{2+} of chlorophyll molecule in LHC, so that LHC can not transfer light energy and the photosynthesis of *P. americana* was further inhibited (Parmar et al. 2013). However, the expression of these 11 LHC genes began to increase at 24 h, and the photosynthesis of *P. americana* began to resume after 48 h.

Cell wall immobilization

Through comparative transcriptome analysis of *P. americana* in response to Cd stress, there were 3 KEGG pathways that showed the most significant enrichment, including flavonoid biosynthesis, phenylpropanoid biosynthesis, and phenylalanine metabolism (Table 3). These 3 metabolic pathways all belong to the phenylpropanoid metabolic pathway, which is a very important secondary metabolic pathway in plants and can generate a wide variety of phenylpropanoid compounds, such as flavonoids, phenolic acids, monolignols, stilbenes, coumarins and lignin (Deng and Lu 2017). These phenylpropanoid compounds play an important role in plant growth and development, cell wall formation, stress tolerance, resistance to pathogen infection, pigment formation, and so on (Vogt 2010). The phenylpropanoid metabolic pathway derives from the phenylalanine produced by the shikimate pathway. Phenylalanine forms *p*-Coumaroyl CoA under the continuous catalysis of phenylalanine ammonia lyase (PAL), C4H, and 4CL. Then *p*-Coumaroyl CoA enters different downstream synthesis pathways of flavonoid, phenolic acid, coumarin and lignin, respectively (Deng and Lu 2017).

Previous researches showed that Cd existed mainly as inorganic ions in the roots of *P. americana*. In the leaves, Cd was combined with pectin and proteins, and was distributed in the cell walls and vacuoles to eliminate the toxicity of Cd (Fu et al. 2011). In this study, genes related to the flavonoid biosynthesis pathway were down-regulated under Cd stress (Table 4, Fig. 6a), while genes involved in the lignin biosynthesis pathway were up-regulated (Table 4, Fig. 6b), indicating that *P. americana* could synthesize more lignin in response to Cd stress. Lignin is mainly present in the cell wall of plant cells. The increase of lignin content can increase the degree of lignification of the cell wall, which can prevent the entry of Cd into cells (Cheng et al. 2014). Moreover, as was reported previously, Cd was combined with pectin and protein in cell wall through immobilization, which further prevented Cd from entering the cytoplasm, and reduced the toxicity of Cd on cells.

Chelation and vacuolar compartmentalization

Some genes related to heavy metal chelation, transport and accumulation were up-regulated in *P. americana* against Cd stress, including nicotianamine synthase (NAS) (c65306), metallothionein-like protein type 3 (MT3) (c29649), phytochelatin synthase (PCS) (c44643), natural resistance-associated macrophage protein 3 (NRAMP3) (c48489), Heavy metal ATPase 3 (HMA3) (c48855), and Heavy metal ATPase 5 (HMA5) (c64219) (Table 5).

NAS can catalyze the formation of nicotianamine (NA) from S-adenosylmethionine (SAM). As a key component of metal ions homeostasis in plants, NA was a metal ion chelator, which can chelate divalent metal ions, such as Mn^{2+}, Zn^{2+}, Cu^{2+}, Fe^{2+}, etc. (Clemens et al. 2013). When the hyperaccumulator plant *S. alfredii* was treated with Cd

Table 5 DGEs related to heavy metal accumulation and tolerance genes in *P. americana*

Gene name	Specific function	KO No. [a]	DEG unigene	Fold change[b]				Regulation
				0 h	2 h	12 h	24 h	
Heavy metal ATPase 3 (HMA3)	HMA3 belongs to P_{1B}-type ATPase subfamily and exhibit Cd-specific transport activity	K01534	c48855	1	2.40	4.60	1.89	Up
Heavy metal ATPase 5 (HMA5)	HMA5 participates Cu compartmentalization and detoxification	K17686	c64219	1	5.68	9.11	21.87	Up
Metallothionein-like protein type 3 (MT3)	MT3 has a high content of Cys[c]. MT3 is related to heavy metal detoxication, and ROS[d] scavenging	-	c29649	1	1.68	2.31	1.44	Up
Phytochelatin synthase (PCS)	PCS plays a key role in the tolerance of plants to heavy metal through the synthesis of PCs, which can chelate heavy metal in vacuole and then transport to the vacuole	K05941	c44643	1	1.06	1.43	0.97	Up
Natural resistance-associated macrophage protein 3 (NRAMP3)	NRAMP3 locates on the membrane of tonoplast and NRAMP3 can transport a variety of heavy metals to vacuole	K12347	c48489	1	2.03	2.85	2.12	Up
Metal tolerance protein (MTP)	MTP is divalent cation transporter and plays a crucial part in plant heavy metal tolerance	K14692	c61692	1	2.31	2.22	3.45	Up
Nicotianamine synthase (NAS)	NAS is a key component of plant metal homeostasis via the synthesis of NA, which can chelate divalent heavy metal ions	K05953	c65306	1	2.28	1.04	3.00	Up
Zn transporter 1 (ZNT1)	ZNT1 is a plasma membrane transporter that can transport Zn but not Cd, Fe, Mn, or Cu into plant cells	K14709	c65693	1	0.64	0.27	0.38	Down
Zn transporter 4 (ZNT4)	ZNT4 may locate in chloroplast and takes part in the transport of Zn in the plastids	K14709	c61336	1	0.45	0.47	0.66	Down
Serine acetyltransferase 1 (SAT1)	SAT1 is a key enzyme in the biosynthesis of Cys in plants and SAT is involved in plant sulfur metabolism	K00640	c65540	1	4.47	4.27	6.43	Up
S-adenosylmethionine synthase (MAT)	MAT catalyzes the production of SAM[e] and participates in Met[f] metabolism. SAM is the active methyl donor	K00789	c63408	1	1.00	0.45	1.07	Up
			c72366	1	2.12	0.60	1.21	Up
Cobalamin-independent methionine synthase (MetE)	MetE catalyzes the formation of Met through transferring the methyl group form tetrahydrofolate (N^e-CH_3-FH_4) to Hcy [g], which is the final step of Met biosynthesis	K00549	c70912	1	1.58	0.46	1.07	Up
Glutathione S-transferase (GST)	GST is involved in heavy metal detoxification through conjugating GSH[h] to heavy metal. GST can improve plant tolerance to heavy metal stress by enhancing the antioxidant system in plants	K00799	c54726	1	3.06	37.07	61.67	Up
			c56713	1	2.11	1.28	2.41	Up
			c68822	1	2.36	1.27	1.00	Up
			c71425	1	1.84	1.40	11.41	Up
			c72656	1	2.56	3.34	4.93	Up

[a]KEGG Orthology (KO) entry

[b]Fold change in comparison with FPKM value at 0 h

[c]*Cys* cysteine

[d]*ROS* reactive oxygen species

[e]*SAM S*-adenosylmethionine

[f]*Met* methionine

[g]*Hcy* homocysteine

[h]*GSH* glutathione

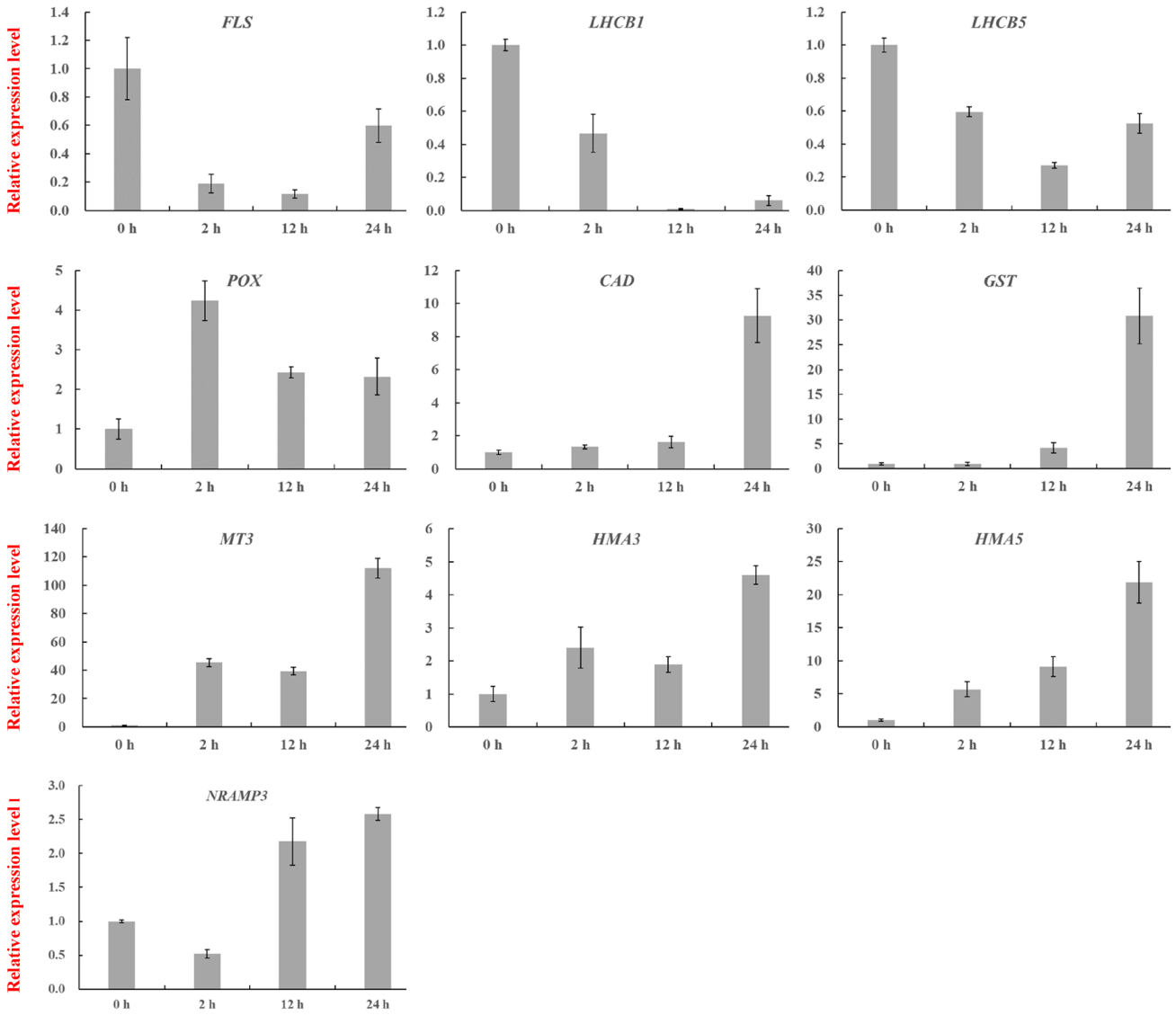

Fig. 7 The expression pattern of genes in the leaves of *P. americana* at different time point after Cd treatment. Transcription levels were verified by qRT-PCR with *PaTUBLIN-α* as an internal control. *FLS*, flavonol synthase; *LHCB1*, light-harvesting complex b1; *LHCB5*, light-harvesting complex b5; *POX*, plant peroxidase; *CAD*, cinnamyl alcohol dehydrogenase; *GST*, glutathione S-transferase; *MT3*, metallothionein-like protein type 3; *HMA3*, heavy metal ATPase 3; *HMA5*, heavy metal ATPase 5; *NRAMP3*, natural resistance-associated macrophage protein 3

or Zn, the expression of *SaNAS* gene was significantly up-regulated and the content of NA also increased. The expression of *SaNAS* gene in yeast can improve the tolerance of yeast to Cd or Zn. The *SaNAS* gene was expressed in *Arabidopsis thaliana*, which can increase the content of NA, and accumulated more Cd or Zn in the roots and aerial parts (Chen et al. 2019). The *NAS* gene expression in the leaves of *P. americana* increased 2.28–3.00 fold after Cd treatment (Table 5), indicating that *P. americana* could produce more NA to cope with Cd stress.

Metallothionein (MT) is an important class of proteins involved in the detoxification of heavy metals in the organisms. As a cysteine (Cys) rich protein with low molecular weight (6-7 kDa), MT is encoded by the *MT* gene family, which can reduce the toxicity of heavy metals, by chelating heavy metals with sulfhydryl group in Cys residues to form MT-heavy metal complex (Cobbett and Goldsbrough 2002). The overexpression of *AtMT3* gene can increase the Cd tolerance of yeast and *Vicia faba* cells (Lee et al. 2004). In the yeast mutant, which is sensitive to Cd/Zn, the expression of the *PaMT2* gene can improve the tolerance of the yeast transformant to Cd (Zhao et al. 2019). The expression of *MT like 3* gene was up-regulated by 1.44–2.31 fold after Cd treatment (Table 5), indicating

the MT played an important role in the detoxification of Cd in *P. americana*.

PCS is able to catalyze GSH to generate phytochelatins (PCs). PCs are also a class of Cys-rich proteins that can chelate heavy metals with sulfhydryl groups to form PC-heavy metal complexes, which are then transported to the vacuole for accumulation (Clemens 2006; Cobbett and Goldsbrough 2002). The expression of PCS gene was up-regulated in *P. americana* under Cd stress. In previous reports, the overexpression of the *AtPCS* gene increased the content of PCs in plants by 2.1 times as compared with wild type (Lee et al. 2003), and promoted the accumulation of Cd in transgenic tobacco (Pomponi et al. 2006). However, the overexpression of *AtPCS* gene did not improve the plant tolerance to Cd, but instead made the plant hypersensitive to Cd and Zn, which may be caused by the toxicity of PCs at supraoptimal concentrations (Lee et al. 2003). The Cd-sensitive mutant of *Schizosaccharomyces pombe* can synthesize PCs, but was unable to accumulate PC-Cd complexes. This phenotype was due to the lack of a *hmt1*gene, which encoded an ABC transporter (Ortiz et al. 1992).

Therefore, increasing the PCs content alone does not improve the plant tolerance to Cd, the capacity to transport the PC-Cd complex into the vacuole also needs to be improved. It has been reported that the heavy metal ion transporters distributed on the plant membrane play an important role in the uptake and transport of heavy metals (Williams et al. 2000).

NRAMP3 was a protein located on the surface of tonoplast (Oomen et al. 2009; Thomine et al. 2003), which was capable of transporting a variety of heavy metals, such as Mn, Zn, Cu, Fe, Cd, etc. (Nevo and Nelson 2006). The *NRAMP* gene was highly expressed in heavy metal hyperaccumulator plants such as *T. caerulescens* and *A. halleri*, and was involved in Cd transport and accumulation.

HMA3 and HMA5 both belonged to P_{1B}-ATPase superfamily, which were located on the tonoplast and were able to transport heavy metals, including Cd, Zn, Co, Pb as well as Cu, into the vacuole for accumulation (Andrés-Colás et al. 2006; Møller et al. 1996). *A. thaliana* mutant with *AtHMA3* gene deletion exhibited sensitive phenotypes to Cd and Zn (Morel et al. 2009). The *SpHMA3* gene of hyperaccumulator plant *S. plumbizincicola* was overexpressed in yeast, which can improve the tolerance of yeast to Cd, and exhibited specific Cd transport activity, while the decrease of *SpHMA3* expression by RNAi led to the hypersensitivity of *S. plumbizincicola* to Cd (Liu et al. 2017). *AtHMA5* played a role in the detoxification and compartmentalization of Cu in *A. thaliana*. The expression level of *AtHMA5* was significantly increased under Cu treatment, and the T-DNA insertion mutants *hma5-1* and *hma5-2* showed hypersensitivity to Cu (Andrés-Colás et al. 2006).

In this study, after Cd treatment, the expression level of NRAMP3, HMA3 and HMA5 were up-regulated by 2.03–2.85 times, 1.89–4.60 times and 5.68–21.87 times respectively. These results indicated that chelation and vacuolar compartmentalization were important mechanisms for the detoxification of Cd in hyperaccumulator plant *P. americana* (Sharma et al. 2016).

Both ZNT1 and ZNT4 were down-regulated in *P. americana* after Cd treatment. These two genes belonged to the cation diffusion facilitator (CDF) gene family (Ricachenevsky et al. 2013), which were mainly involved in the transport and accumulation of Zn in plants, and may not participate in the response of *P. americana* against Cd stress.

Sulfur and GSH metabolism

The genes related to sulfur and GSH metabolism were up-regulated in *P. americana* leaves after Cd treatment, for instance, the expression levels of serine acetyltransferase 1 (SAT1) (c65540), S-adenosylmethionine synthase (MAT) (c72366, c63408) and cobalamin-independent methionine synthase (MetE) (c70912) increased by 4.27–6.43 times, 1.21–2.12 times, and 1.07–1.58 times respectively (Table 5).

These results implied that the accumulation of methionine (Met) and the SAM cycle in *P. americana* were enhanced under Cd stress. As an active methyl donor, SAM provided methyl groups for methylation reactions during plant growth and development, and it was also the precursor of NA, polyamines (PAs) and ethylene biosynthesis in plants (Sauter et al. 2013). SAT1 and the intermediate of the SAM cycle both participated in the formation of Cys, which was an essential substrate for GSH biosynthesis (Droux 2003). The increased expression levels of these genes promoted the biosynthesis of GSH (Mendoza-Cózatl et al. 2005), and increased the content of Cys and GSH in plants (Domínguez-Solís et al. 2004), which may be a protective mechanism against the Cd stress in *P. americana*.

In addition, the expression levels of glutathione S-transferase (GST) (c54726, c56713, c68822, c71425, c72656) genes were significantly up-regulated by 1.27–61.67 times (Table 5). In our previous report, it was found that the abundance of GST proteins in the leaves of *P. americana* increased by 2.09–4.61 fold after Cd treatment (Zhao et al. 2011). GST existed ubiquitously in plants and the expression of *GST* gene was induced by various stress conditions, such as salt, drought, cold, heavy metal, etc. GST can catalyze the covalent binding of GSH with cytotoxic substrates to form glutathione S-conjugates, which were then transferred into vacuolar for compartmentalization (Kumar and Trivedi 2018; Marrs 1996). The reactive oxygen species (ROS) increased under Cd stress and caused oxidative stress to plants (Grobelak et al. 2019). GST was able to catalyze the conjugation of GSH with ROS to quench these ROS,

protecting cells from oxidative damage (Hossain et al. 2012). The GST gene expression level in the leaves of *P. americana* was significantly increased up to 1.27–61.67 times after Cd treatment, indicating that GST played a key role in protecting cells from oxidative stress.

Conclusion

The expression patterns of different functional genes in the leaves of *P. americana* changed after Cd treatment, which was the important molecular basis of Cd tolerance in *P. americana*. In total, 5054 DEGs were obtained through comparative transcriptome analysis. The KEGG pathway enrichment analysis of DEGs indicated that the phenylpropanoid metabolic pathway may be vital for *P. americana* against Cd stress. The flavonoid biosynthesis in the phenylpropanoid metabolic pathway was significantly inhibited, while the lignin biosynthesis was remarkably enhanced. The results indicated that *P. americana* could synthesize more lignin to cope with Cd stress, so as to improve the tolerance of *P. americana* to Cd through cell wall immobilization. Moreover, chelation and vacuolar compartmentalization played an important role in the Cd detoxification of the hyperaccumulator plant *P. americana*. The expression of *LHC* genes in the photosystem reduced significantly under Cd stress, indicating that the photosynthesis sensitivity to Cd existed even in the hyperaccumulator plant. The genes related to sulfur and GSH metabolism were up-regulated, implying that the SAM cycle was enhanced under Cd stress to meet the needs of methyl donors in multiple biosynthesis pathways, at the same time, more Cys and GSH were produced. Therefore, the increase of thiol compounds content might be an important mechanism for *P. americana* to cope with Cd stress. Like other heavy metals, Cd also led to an increase of ROS and caused oxidative stress to cells. The expression level of *GST* gene was significantly up-regulated after Cd treatment, suggesting that *GST* gene may be essential to quench ROS and protect cells from oxidative damage. Moreover, a large number of candidate genes were provided in this study, which can be used to further investigate the molecular mechanism of plant tolerance to Cd.

Supplementary Information The online version contains supplementary material available at https://doi.org/10.1007/s13205-021-02865-x.

Acknowledgements This work was supported by National Key Research and Development Project (2017YFC1702800), Major Science and Technology Project in Henan Province (171100310500), Henan Province Science and Technology Research Project (172102110099) and National College Student's Innovation and Entrepreneurship Training Program (201710471022). We thank Mrs. Kai Tan for assisting in the preparation of this manuscript.

Author's contributions Le Zhao, Yun-hao Zhu, Xing-can Li and Meng-jia Zhang performed the experiments; Min Wang, Yong-guang Han, Li-gang Ma, and Xing-can Li analyzed the data; Meng-jia Zhang conducted the qRT-PCR verification; Le Zhao and Yun-hao Zhu drafted the manuscript; Wei-sheng Feng and Xiao-ke Zheng reviewed the manuscript. All authors have read and agreed to the published version of the manuscript.

Declarations

Conflict of interest The authors declare that they have no conflict of interest.

References

Andrés-Colás N, Sancenón V, Rodríguez-Navarro S, Mayo S, Thiele DJ, Ecker JR, Puig S, Peñarrubia L (2006) The Arabidopsis heavy metal P-type ATPase HMA5 interacts with metallochaperones and functions in copper detoxification of roots. Plant J 45:225–236

Arnon DI (1949) Copper enzymes in isolated chloroplasts. Polyphenoloxidase in *Beta Vulgaris*. Plant Physiol 24:1–15

Baryla A, Carrier P, Franck F, Coulomb C, Sahut C, Havaux M (2001) Leaf chlorosis in oilseed rape plants (*Brassica napus*) grown on cadmium-polluted soil: causes and consequences for photosynthesis and growth. Planta 212:696–709

Bertin G, Averbeck D (2006) Cadmium: cellular effects, modifications of biomolecules, modulation of DNA repair and genotoxic consequences (a review). Biochimie 88:1549–1559

Chen S, Zhang M, Feng Y, Sahito ZA, Tian S, Yang X (2019) Nicotianamine synthase gene 1 from the hyperaccumulator *Sedum alfredii* Hance is associated with Cd/Zn tolerance and accumulation in plants. Plant Soil 443:413–427

Chen Y, Zhi J, Zhang H, Li J, Zhao Q, Xu J (2017) Transcriptome analysis of *Phytolacca americana* L in response to cadmium stress. PLoS ONE 12:e0184681

Cheng H, Jiang ZY, Liu Y, Ye ZH, Wu ML, Sun CC, Sun FL, Fei J, Wang YS (2014) Metal (Pb, Zn and Cu) uptake and tolerance by mangroves in relation to root anatomy and lignification/suberization. Tree Physiol 34:646–656

Clemens S (2006) Evolution and function of phytochelatin synthases. J Plant Physiol 163:319–332

Clemens S, Deinlein U, Ahmadi H, Höreth S, Uraguchi S (2013) Nicotianamine is a major player in plant Zn homeostasis. Biometals 26:623–632

Cobbett C, Goldsbrough P (2002) Phytochelatins and metallothioneins: roles in heavy metal detoxification and homeostasis. Annu Rev Plant Biol 53:159–182

Consortium GO (2004) The Gene Ontology (GO) database and informatics resource. Nucleic Acids Res 32:D258–D261

Cosio C, DeSantis L, Frey B, Diallo S, Keller C (2005) Distribution of cadmium in leaves of *Thlaspi caerulescens*. J Exp Bot 56:765–775

Deng Y, Lu S (2017) Biosynthesis and regulation of phenylpropanoids in plants. Crit Rev Plant Sci 36:257–290

Domínguez-Solís JR, López-Martín MC, Ager FJ, Ynsa MD, Romero LC, Gotor C (2004) Increased cysteine availability is essential for cadmium tolerance and accumulation in *Arabidopsis thaliana*. Plant Biotechnol J 2:469–476

Droux M (2003) Plant serine acetyltransferase: new insights for regulation of sulphur metabolism in plant cells. Plant Physiol Biochem 41:619–627

Eddy SR (1998) Profile hidden Markov models. Bioinformatics 14:755–763

Fagioni M, Zolla L (2009) Does the different proteomic profile found in apical and basal leaves of spinach reveal a strategy of this plant toward cadmium pollution response? J Proteome Res 8:2519–2529

Fu X, Dou C, Chen Y, Chen X, Shi J, Yu M, Xu J (2011) Subcellular distribution and chemical forms of cadmium in *Phytolacca americana* L. J Hazard Mater 186:103–107

Gallego SM, Pena LB, Barcia RA, Azpilicueta CE, Lannone MF, Rosales EP, Zawoznik MS, Groppa MD, Benavides MP (2012) Unravelling cadmium toxicity and tolerance in plants: Insight into regulatory mechanisms. Environ Exp Bot 83:33–46

Gao L, Peng K, Xia Y, Wang G, Niu L, Lian C, Shen Z (2013) Cadmium and manganese accumulation in *Phytolacca americana* L. and the roles of non-protein thiols and organic acids. Int J Phytoremediat 15:307–319

Gong JM, Lee DA, Schroeder JI (2003) Long-distance root-to-shoot transport of phytochelatins and cadmium in *Arabidopsis*. Proc Natl Acad Sci USA 100:10118–10123

Grabherr MG, Haas BJ, Yassour M, Levin JZ, Thompson DA, Amit I, Xian A, Fan L, Raychowdhury R, Zeng Q (2011) Full-length transcriptome assembly from RNA-Seq data without a reference genome. Nature Biotechnol 29:644–652

Grobelak A, Świątek J, Murtaś A, Jaskulak M (2019) Chapter 9 - Cadmium-Induced oxidative stress in plants, cadmium toxicity, and tolerance in plants: from physiology to remediation. In: Hasanuzzaman M, Prasad MNV, Fujita M (eds) Cadmium toxicity and tolerance in plants. Academic Press, pp 213–231

Hoagland DR, Arnon DI (1950) The water-culture method for growing plants without soil. California Agricultural Experiment Station Circular 347:30–32

Hossain MA, Piyatida P, da Silva JAT, Fujita M (2012) Molecular mechanism of heavy metal toxicity and tolerance in plants: central role of glutathione in detoxification of reactive oxygen species and methylglyoxal and in heavy metal chelation. J Bot 2012:872–875

Jiang J, Wu L, Li N, Luo Y, Liu L, Zhao Q, Zhang L, Christie P (2010) Effects of multiple heavy metal contamination and repeated phytoextraction by *Sedum plumbizincicola* on soil microbial properties. Eur J Soil Biol 46:18–26

Jin X, Shi C, Yu CY, Yamada T, Sacks EJ (2017) Determination of leaf water content by visible and near-infrared spectrometry and multivariate calibration in *Miscanthus*. Front Plant Sci 8:721

Kanehisa M, Goto S (2000) KEGG: kyoto encyclopedia of genes and genomes. Nucleic Acids Res 28:27–30

Krämer U (2010) Metal hyperaccumulation in plants. Annu Rev Plant Biol 61:517

Kumar S, Trivedi PK (2018) Glutathione S-Transferases: role in combating abiotic stresses including arsenic detoxification in plants. Front Plant Sci 9:751

Lane TW, Morel FMM (2000) A biological function for cadmium in marine diatoms. Proc Natl Acad Sci USA 97:4627–4631

Langmead B, Trapnell C, Pop M, Salzberg SL (2009) Ultrafast and memory-efficient alignment of short DNA sequences to the human genome. Genome Biol 10:R25

Lee J, Donghwan S, Won-yong S, Inhwan H, Youngsook L (2004) Arabidopsis metallothioneins 2a and 3 enhance resistance to cadmium when expressed in *Vicia faba* guard cells. Plant Mol Biol 54:805–815

Lee S, Moon JS, Ko T-S, Petros D, Goldsbrough PB, Korban SS (2003) Overexpression of Arabidopsis phytochelatin synthase paradoxically leads to hypersensitivity to cadmium stress. Plant Physiol 131:656–663

Liu XQ, Peng KJ, Wang AG, Lian CL, Shen ZG (2010) Cadmium accumulation and distribution in populations of *Phytolacca americana* L. and the role of transpiration. Chemosphere 78:1136–1141

Liu H, Zhao H, Wu L, Liu A, Zhao F-J, Xu W (2017) Heavy metal ATPase 3 (HMA3) confers cadmium hypertolerance on the cadmium/zinc hyperaccumulator *Sedum plumbizincicola*. New Phytol 215:687–698

Livak KJ, Schmittgen TD (2001) Analysis of relative gene expression data using real-time quantitative PCR and the $2^{-\Delta\Delta CT}$ method. Methods 25:402–408

Luo ZB, He J, Polle A, Rennenberg H (2016) Heavy metal accumulation and signal transduction in herbaceous and woody plants: paving the way for enhancing phytoremediation efficiency. Biotechnol Adv 34:1131–1148

Marrs KA (1996) The functions and regulation of glutathione s-transferases in plants. Annu Rev Plant Physiol Plant Mol Biol 47:127–158

McBride MB, Zhou Y (2019) Cadmium and zinc bioaccumulation by *Phytolacca americana* from hydroponic media and contaminated soils. Int J Phytoremediation 21:1215–1224

Mendoza-Cózatl D, Loza-Tavera H, Hernández-Navarro A, Moreno-Sánchez R (2005) Sulfur assimilation and glutathione metabolism under cadmium stress in yeast, protists and plants. FEMS Microbiol Rev 29:653–671

Ministry of Environmental Protection, Ministry of Land and Resources (2014) National soil pollution survey Bulletin; 2014 Apr 17. Available from: http://www.mee.gov.cn/gkml/sthjbgw/qt/201404/W020140417558995804588.pdf (In Chinese).

Morel M, Crouzet J, Gravot A, Auroy P, Leonhardt N, Vavasseur A, Richaud P (2009) AtHMA3, a P_{1B}-ATPase allowing Cd/Zn/Co/Pb vacuolar storage in Arabidopsis. Plant Physiol 149:894–904

Murashige T, Skoog F (1962) A revised medium for rapid growth and bio assays with tobacco tissue cultures. Physiol Plant 15:473–497

Møller JV, Juul B, le Maire M (1996) Structural organization, ion transport, and energy transduction of P-type ATPases. BBA-Rev Biomembranes 1286:1–51

Neller KCM, Klenov A, Hudak KA (2016) The pokeweed leaf mRNA transcriptome and its regulation by jasmonic acid. Front Plant Sci 7:283

Nevo Y, Nelson N (2006) The NRAMP family of metal-ion transporters. BBA Mol Cell Res 1763:609–620

Oomen RJFJ, Wu J, Lelièvre F, Blanchet S, Richaud P, Barbier-Brygoo H, Aarts MGM, Thomine S (2009) Functional characterization of NRAMP3 and NRAMP4 from the metal hyperaccumulator *Thlaspi caerulescens*. New Phytol 181:637–650

Ortiz DF, Kreppel L, Speiser DM, Scheel G, McDonald G, Ow DW (1992) Heavy metal tolerance in the fission yeast requires an ATP-binding cassette-type vacuolar membrane transporter. EMBO J 11:3491–3499

Parmar P, Kumari N, Sharma V (2013) Structural and functional alterations in photosynthetic apparatus of plants under cadmium stress. Bot Stud 54:45

Peng K, Luo C, You W, Lian C, Li X, Shen Z (2008) Manganese uptake and interactions with cadmium in the hyperaccumulator—*Phytolacca Americana* L. J Hazard Mater 154:674–681

Pilon-Smits E (2005) Phytoremediation. Annu Rev Plant Biol 56:15–39

Pomponi M, Censi V, Di Girolamo V, De Paolis A, di Toppi LS, Aromolo R, Costantino P, Cardarelli M (2006) Overexpression of Arabidopsis phytochelatin synthase in tobacco plants enhances Cd^{2+} tolerance and accumulation but not translocation to the shoot. Planta 223:180–190

Qadir S, Jamshieed S, Rasool S, Ashraf M, Akram NA, Ahmad P (2014) Modulation of plant growth and metabolism in cadmium-enriched environments. In: D. W (Eds) Reviews of environmental contamination and toxicology. Springer, pp 51–88

Rascio N, Navariizzo F (2011) Heavy metal hyperaccumulating plants: how and why do they do it? And what makes them so interesting? Plant Sci 180:169–181

Ricachenevsky F, Menguer P, Sperotto R, Williams L, Fett J (2013) Roles of plant metal tolerance proteins (MTP) in metal storage and potential use in biofortification strategies. Front Plant Sci 4:144

Satarug S, Garrett SH, Sens MA, Sens DA (2010) Cadmium, environmental exposure, and health outcomes. Environ Health Perspect 118:182–190

Sauter M, Moffatt B, Saechao Maye C, Hell R, Wirtz M (2013) Methionine salvage and S-adenosylmethionine: essential links between sulfur, ethylene and polyamine biosynthesis. Biochem J 451:145–154

Sharma SS, Dietz K-J, Mimura T (2016) Vacuolar compartmentalization as indispensable component of heavy metal detoxification in plants. Plant Cell Environ 39:1112–1126

Thomine S, Lelièvre F, Debarbieux E, Schroeder JI, Barbier-Brygoo H (2003) AtNRAMP3, a multispecific vacuolar metal transporter involved in plant responses to iron deficiency. Plant J 34:685–695

Trapnell C, Williams BA, Pertea G, Mortazavi A, Kwan G, van Baren MJ, Salzberg SL, Wold BJ, Pachter L (2010) Transcript assembly and quantification by RNA-Seq reveals unannotated transcripts and isoform switching during cell differentiation. Nature Biotechnol 28:511–515

Verbruggen N, Hermans C, Schat H (2009) Molecular mechanisms of metal hyperaccumulation in plants. New Phytol 181:759

Vogt T (2010) Phenylpropanoid biosynthesis. Mol Plant 3:2–20

Wang X, Zhao H, Liu H, Cai T (2012) Expression analysis of *PaMT* from *Phytolacca americana* (In Chinese). J Graduate Univer Chinese Acad Sci 29(4):449–454

Wei L, Shu W, Lan C (2004) *Viola baoshanensis*, a plant that hyperaccumulates cadmium. Sci Bull 49:29–32

Williams LE, Pittman JK, Hall JL (2000) Emerging mechanisms for heavy metal transport in plants. BBA Biomembranes 1465:104–126

Xie C, Mao X, Huang J, Ding Y, Wu J, Dong S, Kong L, Gao G, Li CY, Wei L (2011) KOBAS 2.0: a web server for annotation and identification of enriched pathways and diseases. Nucleic Acids Res 39:W316–W322

Yan H, Filardo F, Hu X, Zhao X, Fu D (2016) Cadmium stress alters the redox reaction and hormone balance in oilseed rape (*Brassica napus* L.) leaves. Environ Sci Pollut Res 23:3758–3769

Zhao L, Sun YL, Cui SX, Chen M, Yang HM, Liu HM, Chai TY, Huang F (2011) Cd-induced changes in leaf proteome of the hyperaccumulator plant *Phytolacca americana*. Chemosphere 85:56–66

Zhao H, Wei Y, Wang J, Chai T (2019) Isolation and expression analysis of cadmium-induced genes from Cd/Mn hyperaccumulator *Phytolacca americana* in response to high Cd exposure. Plant Biol 21:15–24

Šimonová E, Henselová M, Masarovičová E, Kohanová J (2007) Comparison of tolerance of *Brassica juncea* and *Vigna radiata* to cadmium. Biol Plant 51:488–492